Mechanical Properties and Microstructural Properties of CrSiN Coating

Dhiflaoui Hafedh, Khlifi Kaouthar, Ben Cheikh Larbi Ahmed

Abstract—The present study deals with the characterization of CrSiN coatings obtained by PVD magnetron sputtering systems. CrSiN films were deposited with different Si contents, in order to check the effect of at.% variation on the different properties of the Cr–N system. Coatings were characterized by scanning electron microscopy (SEM) for thickness measurements, X-ray diffraction. Surface morphology and the roughness characteristics were explored using AFM, Mechanicals properties, elastic and plastic deformation resistance of thin films were investigated using nanoindentation test.

We observed that the Si addition improved the hardness and the Young's modulus of the Cr–N system. Indeed, the hardness value is 18,56 GPa for CrSiN coatings. Besides, the Young's modulus value is 224,22 GPa for CrSiN coatings for Si content of 1.2 at.%.

Keywords—Thin film, mechanicals properties, PVD.

I. INTRODUCTION

TECHNIQUES used to produce thin films are developed leading to an improvement of the performance and durability of precision components. Physical vapor deposition (PVD) is one of the most developed technologies through its contribution to the improvement of mechanical properties of thin films. It allowed the fabrication of a multitude of metal nitride, carbide, and oxide coatings. Chromium nitride (CrN) coatings is a well-known thin film that have been proposed to be a promising hard coating material owing to its high hardness, wear, corrosion and high temperature oxidation resistance [1]-[3].

In the recent years, various efforts have been made to improve their mechanical, tribological and oxidation resistance for the industrial applications, such as machining, forming, casting and other mechanical applications by the incorporation of other elements, such as Al, Mo, C, V and W [4], [5].

It has been reported that the addition of Al in CrN and TiN films have modified their structural, mechanical and tribological properties [6]. The addition of silicon (Si) into the CrN has been founded as a solution to improve the mechanical and tribological properties [7]-[10]. The hardness (H) and modulus (E) of the sputtered CrSiN coatings, with 2.3 at.% silicon content, measured, by using depth sensing indentation were found to be 24 GPa and 240 GPa, respectively [11].

Lee and Chang [12] have reported that the surface roughness, grain size, hardness, and friction coefficient of pulsed DC-reactive magnetron sputtered CrSiN coatings

Dhiflaoui Hafedh, Khlifi Kaouthar, and Ben C. L. Ahmed are with Laboratoire Mécanique Matéériaux et Procédés, Ecole Supeérieure des Sciences et Techniques de Tunis, University of Tunis, Tunisia (e-mail: dhafedh@gmail.com).

decreases with increasing Si contents from 0.7 to 12.9 at.%. They have reported high hardness (24.6 GPa), low friction coefficient, and high wear resistance, for the CrSiN coatings containing 10.0 at.% Si. Furthermore, some authors discussed the influence of reactive gas and temperature on structural properties of magnetron sputtered CrSiN coatings [13]. But a very few works focused on the effect of this incorporation of silicon (Si) on the adhesion quality, whereas a thin film that does not adhered to its substrate is of any importance. The present work have been focused to study the microstructural characteristics and the adhesion of CrSiN coatings deposited on XC100 steel, under different bias voltages of the silicon target and compared to the CrAlN.

II. EXPERIMENTAL PROCEDURE

A. Films Deposition

CrAlN and CrSiN films were deposited on XC 100 steel substrates by medium frequency magnetron sputtering. The separately applied targets are Cr (99.99%) and Si (99.99%). The films were deposited in Ar and N2 mixture introduced into the deposition chamber. Before the deposition, the substrates are ultrasonic-cleaned using acetone and ethanol. The experiments are done with different Si content. The CrN films are also deposited as the reference. The Si contents in the films are controlled by the input direct current (DC) from 0.4A to 2.4A. The base pressure in the deposition chamber is 2 x 10-3 Pa, while the total pressure of N2 and Ar during the CrSiN deposition is adjusted to 1.0 Pa. The ratio of Ar/ N2 mixture is 1:3 during the deposition. A layer of pure Cr (for 10 min in Ar atmosphere) is deposited as the transition layer on the substrates to improve the adhesion. Then CrSiN is deposited on the substrates for four hours.

B. Films Characterization

The coating surface structure was examined using scanning electron microscopy (SEM). Crystal structure of the coatings is investigated by Panalytical X'pert PRO X-ray diffraction (XDR, Philips, Netherlands) using Cu Kα radiation as X-ray source. Surface morphology and the roughness characteristics are explored using AFM in contact mode, high resonance frequency SiN cantilevers, with a pyramidal tip of 50 nm radius and a force constant of 0.032 N/m. Mechanicals properties, elastic and plastic deformation resistance of thin films were investigated using nanoindentation test, which were performed in a nanoindenter developed by CSM instruments Switzerland, using a diamond Berkovich tip under a maximum load of 50mN. At this load, the indentation depth is much less than 1/10th of the film thickness, thus minimizing

Also

World Academy of Science, Engineering and Technology
International Journal of Materials and Metallurgical Engineering
Vol:9, No:8, 2015

the effect of substrate on the hardness measurements [14]. Results are averaged over more than 10 measurements.

III. RESULTS AND DISCUSSION

A. X-ray Diffraction (XDR)

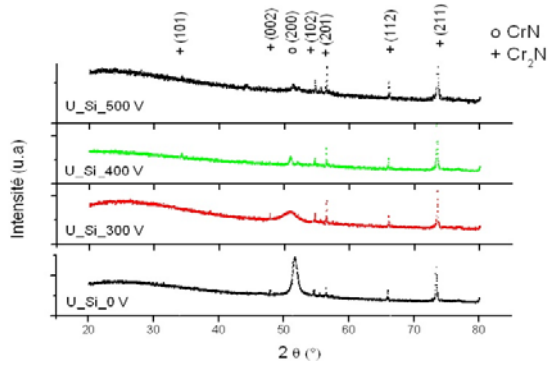Results of X-ray diffraction are shown in Fig. 1.

Fig. 1 X-ray diffraction patterns of CrSiN and CrAlN thin film

For the CrSiN, when the bias voltage is 0 V, the diffraction of the cubic phase of CrN is observed with a characteristic peak of the planes (200) at 51.2° and 74.07° Cr2N phase according to the plans (211), we have also observed other diffractions of other plans, Cr2N line with lower intensities from the CrN phase. These planes (002), (102), (201) and (112) diffract theoretically to angles 47.64°, 54.6°, 56.55° and 66.19° respectively.

The application of a voltage to the silicon target, followed by the addition of silicon in the layer of CrN, which result in a phase transformation observed on diffractogram USi = -300 V. Indeed, we notice that the peak associated with the cubic CrN phase become broader and less intense. This indicates a change in the structure level accompanied by more intense peaks related to Cr2N phase. For a voltage applied, to the silicon target USi = -400 V, we notice a significant decrease in intensity of the cubic phase CrN, and the generation of a new direction in Cr2N phase (101) to 34 °. With USi = - 500 V, it is observed that the peak on the cubic phase is less intense. Other peaks correspond to the hexagonal phase Cr2N having the crystal orientations (201) and (211) as the most intense. The diffractogram of the CrAlN layer offers major peaks along the lines (111), (200) and (220) which are identical to those of the CrN phase. Thus, the structure of the CrAlN layer can be likened to that of the cubic phase CrN NaCl-type.

B. Scanning Electron Microscopy (SEM)

Fig. 2 shows the SEM micrographs of CrSiN coatings with variation of the bias voltages of the silicon target.

It is clear that all coatings have a columnar structure and a surface dominated by micro-pores even nanopores. But we have noted a difference in the size of this pore. This result has been confirmed by AFM observation as it's shown in Fig. 3.
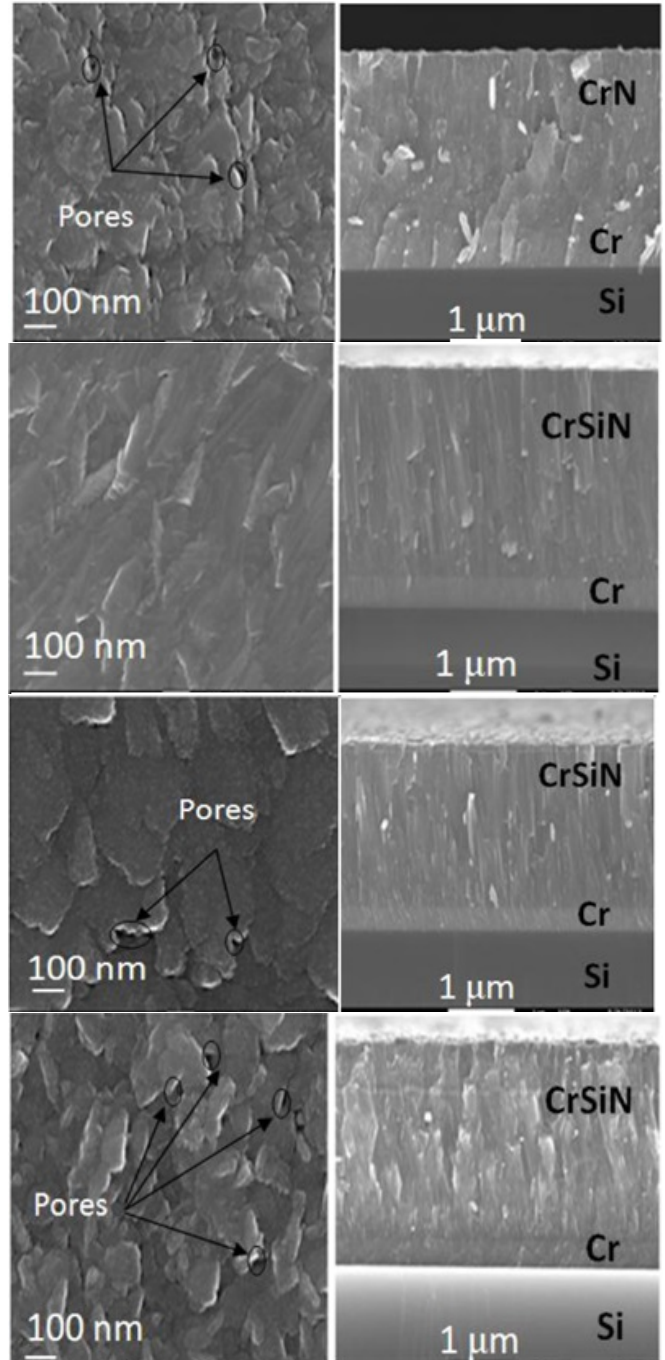

Fig. 2 SEM surface morphology of the films: (a,b) Usi = 0V, (c,d) Usi = -300V, (e,f) Usi = -400V and (g,h) Usi = -500V

World Academy of Science, Engineering and Technology
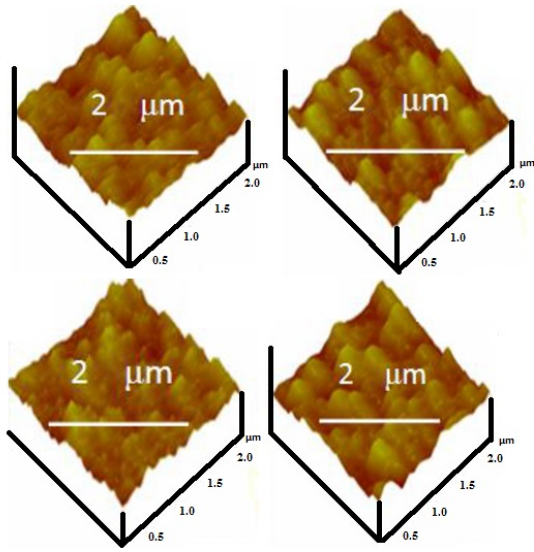International Journal of Materials and Metallurgical Engineering
Vol:9, No:8, 2015

Fig. 3 Three-dimensional AFM images of CrSiN coatings

The AFM examination revealed the presence of domes and craters which are uniformly distributed over the surface. However, we have noticed a difference in the size of the domes and craters that characterizes the morphology as is shown in Fig. 3. Grains size is calculated and the results are illustrated in Table I.

TABLE I
EFFECT OF POLARIZATION ON SI PERCENTAGE AND GRAIN SIZE

Coatings	Polarization USi (V)	Percentage of Si (% at)	Grain size (nm)
CrN	0	0	176
CrSiN	-300	1,2	111
CrSiN	- 400	4,7	109
CrSiN	-500	10,6	143

Results of AFM observation show that the morphology, the roughness and the growth of grains surface was affected by the addition of silicon.

The increase of negative bias voltage to an increase of percentage of Si gives a decrease of the grain size values. Indeed, the film of CrN (0 at.% Si) is constituted of grains with pyramidal facets whose size is of about 176 nm. The grains are elongated when silicon is added (1.2 at.%) In the CrxNy matrix, and thereafter their size decrease to 111 nm.

For higher silicon content, it is observed that the grains are flattened; it is the effect of the energy of deformation in the modified structure model. When the target polarization is about -500 V, a saturation level of silicon to 10.6 at% is observed implying a structural transformation.

The cross sections show a dense and compact growth state. This state density increases with the addition of silicon. Although, the mode of growth is columnar, the state of defects (pores) is minimal according to the surface images of the layers. The layers of CrN and those containing 1.2 at.% and higher of Si have micropores. Yoo et al. [15] have observed a reduction of the porosity of state according to the silicon content in the layers, and have attributed this improvement in

the phase transformation from hexagonal Cr2N (111) CrN (200). The fact that we get the opposite result is therefore explained by the transition from a cubic phase to a mixture CrN + Cr2N, by increasing the rate of Si in our layers, thus, we have only hexagonal Phase at 10.6% at. of Si.

The RMS roughness decreases regularly as a function of silicon content present in the layer as shown in Fig. 4. We also observe on the images that the surface of the layer becomes smoother when the silicon content is higher (10.6 at.%) which may indicate the presence of an amorphous phase in SiNx. Shah et al. [16] have attributed the surface morphology to the segregation of the large fraction of the amorphous phase SiNx in the grain boundaries during film growth.

IV. INSTRUMENTED INDENTATION HARDNESS TESTING

Measuring by nanoindentation requires implementing and monitoring loads as low as a few tens of micro-Newtons, because this technique is used to evaluate the mechanical properties of thin films, without substrate influence. The output from a nanoindentation test is a graph relating the applied load, and the corresponding indenter displacement during the loading and unloading phases. The analysis of these load–displacement graphs with the Oliver and Pharr method [17] lead to the estimation of the mechanical properties (Young's modulus, Hardness of the film). A typical load–displacement curve of CrSiN is shown in Fig. 5. In thus latter, during indentation, hr is the final unloading depth which is obtained when the indenter is completely removed; hmax is the maximum loading depth, Pmax is the maximum load. The area covered under A–B–D–A represents plastic deformation energy (Wp) while area covered under D–B–C–D represents elastic recovery energy (We) during indentation process.
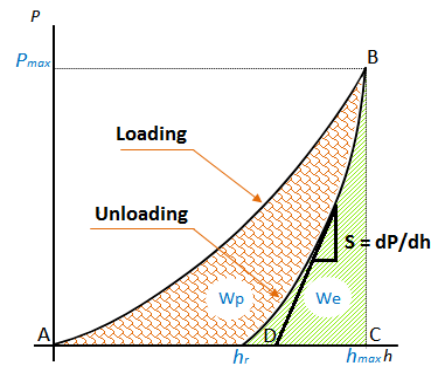

Fig. 4 A typical load–displacement curve

During unloading, the penetration depth decreases with the applied load, and when the indenter is completely removed, the residual depth hf is obtained. S is the contact stiffness (dP/dh) at the maximum load.

$$S = \beta \frac{2}{\sqrt{\pi}} E_{eff} \sqrt{A_C} \qquad (1)$$

where A(hc) stands for the projected contact area of the indenter tip.

World Academy of Science, Engineering and Technology
International Journal of Materials and Metallurgical Engineering
Vol:9, No:8, 2015

The Young's modulus of coating E is calculated from Hertzian equation:

$$\frac{1}{E_{eff}} = \frac{1-\vartheta^2}{E} + \frac{1-\vartheta i^2}{E_i} \qquad (2)$$

where v_i and v are the Poisson's ratios for the indenter and coating, respectively; $E_{indenter}$ and E is the Young's modulus for indenter and coating, respectively. In this study, it is assumed that $v_i = 0.07$ and $E_i = 1140$ GPa for the diamond indenter; and the poison's ratio for the coating materials is assumed to be 0.3.

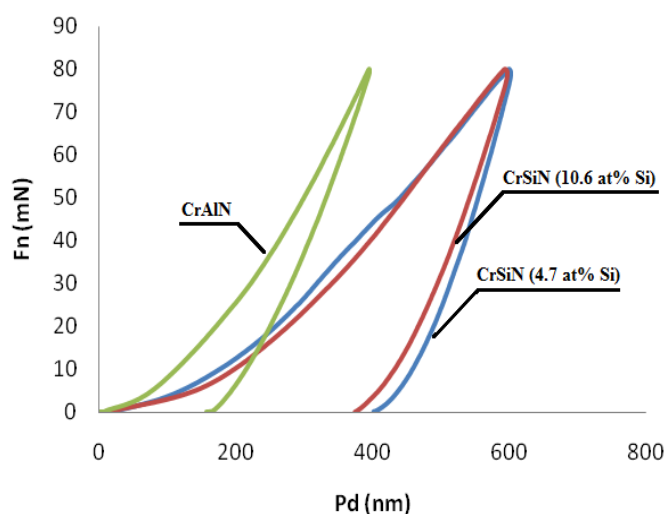Fig. 5 shows load–displacement curves of CrSiN with a variation of target polarization.

Fig. 5 Loading-unloading curve for thin films

For all of the coatings, the loading-unloading curve shows the first part to be in the increase in the penetration depth as a function of the load, the plastic deformation will occur when the maximum load (Pmax), will reach to a maximum penetration depth (hmax).

From these curves, the corresponding composite Young's modulus and hardness values is calculated see Table II. This latter, also gives the corresponding values of the uncoated tool materials and the TiAlN coating.

TABLE II
MECHANICAL PROPERTIES OF THE LAYERS OF CRSIN AS A FUNCTION SILICON RATE

Polarization (V)	%. Si	H (GPa)	E (GPa)	H/E	H3/E*2(GPa)
0	0	10.21	169.72	0.06	0.03
-250	0,7	17.73	182.5	0.09	0.16
-300	1,2	18.56	224.22	0.08	0.12
-400	4,7	17.94	193.05	0.09	0.15
-500	10,6	18.34	172.06	0.1	0.3

First, we are interested to check the influence of the voltage applied to the Si target setting that of Cr. It is noted that the introduction of a slight amount of silicon (0.7 at.%) increases the mechanical properties of the layer. Indeed, the hardness and the modulus of elasticity increase from 10.21 and 169.72

GPa for a layer, whose silicon content is equal to 0% (CrN layer) to 17.73 and 182.5 GPa respectively.

When the silicon content increases, the hardness and the modulus of elasticity increase to reach a maximum of 18.56 GPa and 224.22 GPa for a bias on the target USi = -300 V and Ucr = - 900 V or a silicon rate 1.2% at. Thus, checks what is observed in the previous paragraph: the layer containing 1.2 at.% Si is the densest effect and shows no pore, so this is the hardest, the most stress and more resistant to plastic deformation. Indeed, we note that for the layer, the rate of Si equal to 1.2 at.%, A compressive stress state is quite high (-4 GPa) when compared with a layer of CrN (-0, 8 GPa). These compressive stresses are thereby breaking the movement of defects in the crystal lattice causing a resistance to plastic deformation.

The evolution of the ratio H3/E*2 based on the content of the deposit in layers allows to check the resistance to plastic deformation of the coatings. A high ratio for a given layer means that it has a good ability to delay the plastic deformation, and a good wear resistance.

By examining the results shown in Table II, it is discovered that this ratio can vary from 0.03 to 0.133 depending on the silicon content in the layers of CrSiN. It is well verified that the layer containing 1.2% at. Si has the highest ratio and a good resistance to plastic deformation.

V. CONCLUSIONS

CrSiN coatings thin films are deposited on XC 100 steel with Si contents ranging from 0.7 to 10.6 at.%. microstructural and morphological properties of CrSiN coatings thin films are discovered using scanning electron microscopy (SEM) for thickness measurements, X-ray diffraction and atomic force microscopy AFM, Mechanicals properties, elastic and plastic deformation resistance of thin films are discovered too using nanoindentation test. Mechanical proprieties of Cr-N system depend largely on the quantity of Si. It is found an improvement of the mechanical behavior with the addition of Si (0.7at.%). The best proprieties of coatings are obtained for Si 1.2at.% (Hardness is in the order of 18.56Gpa and Young's modulus is about 224.22 Gpa).

REFERENCES

[1] G. Bertrand, C. Savall, C. Meunier, "Properties of reactively RF magnetron-sputtered chromium nitride coatings," Surface and Coatings Technology vol. 96, 1997, pp. 323-329.
[2] D. Lee, Y. Lee, S. Kwon "High temperature oxidation of a CrN coating deposited on a steel substrate by ion plating," in Surface and Coatings Technology vol. 141, 2001, pp. 227-231.
[3] Z. Han, J. Tian, Q. Lai, X. Yu, G. Li, "Effect of N2 partial pressure on the microstructure and mechanical properties of magnetron sputtered CrNx," in in Surface and Coatings Technology, vol. 162, 2003, pp. 189-193.

World Academy of Science, Engineering and Technology
International Journal of Materials and Metallurgical Engineering
Vol:9, No:8, 2015

[4] Holger Hoche, Stefan Groß, Matthias Oechsn, "Development of new PVD coatings for magnesium alloys with improved corrosion properties," in Surf. Coat. Technol, vol. 259, 2014, pp 102-108.

[5] D.S. Belov, I.V. Blinkov, A.O. Volkhonskii, "The effect of Cu and Ni on the nanostructure and properties of arc-PVD coatings based on titanium nitride," in Surf. Coat. Technol, vol. 260, 2014, pp 186-197.

[6] A. Kimura, M. Kawate, H. Hasegawa, T. Suzuki, "Anisotropic lattice expansion and shrinkage of hexagonal TiAlN and CrAlN films," Surf. Coat. Technol, vol. 367, 2003, pp 169-170.

[7] Lee S-Y, Hong Y-S, "Effect of CrSiN thin film coating on the improvement of the low-speed torque efficiency of a hydraulic piston pump," in Surf. Coat. Technol, vol. 202, 2007, pp 1129-1134.

[8] Yoo YH, Hong JH, Kim JG, Lee HY, Han JG, "Effect of Si addition to CrN coatings on the corrosion resistance of CrN/stainless steel coating/substrate system in a deaerated 3.5 wt.% NaCl solution," in Surf. Coat. Technol, vol. 201, 2007, pp 9518-9523.

[9] Barshilia HC, Selvakumar N, Deepthi B, Rajam KS, "A comparative study of reactive direct current magnetron sputtered CrAlN and CrN coatings," in Surf. Coat. Technol. vol. 201, 2006, pp 2193.

[10] Ding XZ, Zeng XT, "Structural, mechanical and tribological properties of CrAlN coatings deposited by reactive unbalanced magnetron sputtering," in Surface & Coatings Technology, vol. 200, 2005, pp 1372–1376.

[11] Benkahoul M, Robin P, Gujrathi SC, Martinu L, Klemberg-Sapieha JE, "Microstructure and mechanical properties of Cr–Si–N coatings prepared by pulsed reactive dual magnetron sputtering.," in Surf. Coat. Technol. vol. 202, 2008, pp 3975-3980.

[12] Lee J-W, Chang Y-C, "A study on the microstructures and mechanical properties of pulsed DC-reactive magnetron sputtered Cr–Si–N nanocomposite coatings," in Surface & Coatings Technology, vol. 202, 2007, pp 831–835.

[13] Hetal N. Shaha, B. R. Jayaganthana, Davinder Kaurc, "Influence of reactive gas and temperature on structural properties of magnetron sputtered CrSiN coatings," in Applied Surface Science, vol. 257, 2011, pp 5535–5543.

[14] Zenghu H, Jiawan T, Jijun L, Geyang L, Jiawei D, "Effects of thickness and substrate on the mechanical properties of hard coatings," in J. Coat. Technol. Res, vol. 1, 2004, pp 337–341.

[15] Y.H. Yoo, J.H. Hong, J.G. Kim, H.Y. Lee, J.G. Han, "Effect of Si addition to CrN coatings on the corrosion resistance of CrN/stainless steel coating/substrate system in a deaerated 3.5 wt.% NaCl solution," in Surface and Technology, vol. 201, 2007, pp 9518–9523.

[16] Hetal N. Shaha,b, R. Jayaganthana,, Davinder Kaurc, "Influence of reactive gas and temperature on structural properties of magnetron sputtered CrSiN coatings," in Applied Surface Science, vol. 257, 2011, pp 5535–5543.

[17] W. C. Oliver and G. M. Pharr, "An improved technique for determining hardness and elastic modulus using load and displacement sensing indentation experiments," in J. Mater. Res., vol. 6, 1992, pp 1564–1583.